DOI 10.31489/2023No2/57-64

UDC 620.9

ON ASSESSING THE EFFECTIVENESS OF HYBRID SOLAR COLLECTORS SCHEME IN IRAQ'S ENVIRONMENT

Jaddoa, Ameer A.***,** Mahdi Mahmoud M., Hamad Karema A.

Electromechanical Engineering Department, University of Technology, Baghdad, Iraq
ameer.a.jaddoa@uotechnology.edu.iq

An evaluation of the performance of the Iraqi environments in terms of electrical, thermal and exergy efficiency is introduced in this study. The research is carried out in May 2022, in the Baghdad metropolis. The extraction process of heat from the photovoltaic units which arises from the coolant liquid mass flow rate deem as an essential point. The experimental studies were implemented by absorbing heat energy behind from the photovoltaic cell's surface in insulated conditions and using a cooled water unit. The results indicated that at a mass inflow rate of 0.2 kg/sec, the maximum average total efficiency of the system was recorded 22%. As a result, it is advised that to reduce the payback interval, it is possible to design efficient solar photovoltaic–thermal systems to promote the whole system's efficiency and lower the payback interval.

Keywords: Solar Energy, Energy and Exergy, Hybrid Solar PV/T Collector.

Introduction

Renewable energy become an indispensable resource due to several challenges represented by increasing energy cost production, the population rising comes with increases in the power demand notably the limitation of fossil fuel resources. All of these reasons motivated the researchers to search on finding for alternating energy resources. Renewable energy is characterized by low cost. One of the outstanding sustainable energy resources is solar power. In this vein, it can be classified into two kinds of resources thermal and photovoltaic energies in other words conversion of solar power into thermal and electric energy, respectively. Generally, in energy applications, these systems PV and thermal are applied separately; however, it can adopt both simultaneously. It is noteworthy that such schemes (PV/T) have an energy efficiency greater than that of PV and solar thermal techniques as endorsed in the literature by several scholars. In this regard, the authors in [1] presented a new technique called BIPV/T aiming to drop the power consumption in the facilities. In accordance with the results, the authors claimed that an efficiency of 7.6% could be administered in terms of passive cooling in the summer, while about 12.5% was provided in winter. Previous studies have reported that to improve a PV system efficiency cooled with nano-fluids employing an adaptation technique called neuro-fuzzy inference system (ANFIS), the factors of solar irradiation, the nano-fluid inflow rate, and various parameters of nano-fluids were investigated [2]. More recent attention has focused on a BIPV/T approach comprising the phase alternating of material or so-called phase change material (PCM). Such a study was conducted based in Tehran, the capital of Iran. The research reported that the optimal thickness of PCM was measured to be 77.2 mm. Much of the available literature on the payback period deals with the question of period reduction. Renewable energy resources can reduce the annually emitted of CO_2 by 3.3 years of energy payback period. Besides that, a controlling load technique could apply by load OFF-ON according to energy demand along with energy storage unit aiming to expense operation reduction. On the other hand, the micro-grid could control the energy between the power network and the upstream grid, wherein several approaches were proposed to model energy management toward declining the expense operation [4-7]. More recent attention has focused on the light into electricity conversion unit combined with the airflow as a coolant system [8]. In addition to geometrical design, the work emphasised cell temperature, solar intensity, and mass inflow rate (MFR). The primary object was to enhance energy production. Various parameters were studied to investigate the hybrid schemes behavior based on different approaches applied in the simulation processes [9,10]. In this context, the author in [11] used Matlab simulation to validate the water-cooled unit with the outdoor conditions model. In transient conditions, the system PV/T provided an acceptable performance regarding the outlet temperature data. According to the

results, the system response was quick to the change in wind speed. The RMSD for outlet temperature and Pel were 2.07%, and 4.15%, respectively as recorded in May.

Previous studies in [12] have reported introducing a novel method of a water-cooled PV/T strategy composed of a Toddler layer mounted with water tubes organized in parallel form. In conclusion, the research revealed that thermal efficiency dropped to 40% out of 70% upon the increase in wind speed. Based on a 3-dimensional prototype applied to a polymer (3-hexylthiophene), the authors in [13] introduced an analytical module for a hybrid solar collector utilizing Matlab software and Comsol v.5.4. In comparison between polymer-based PV/T prototype monocrystalline-silicon-based PV/T collector units it is found that the first module has 6.57% lower and 85.77% higher for electrical efficiency and thermal efficiency, respectively. In this context, for PV/T systems, a development was introduced based on physical quasi-Steady thermal and transient thermal. The results appeared that both modules achieved identical results. Further, the systems were greatly influenced by the temperature.

The scholars considered that the TRNSYS tool might be the most suitable instrument for the simulation of energy systems. The reason is that it has the capability to simulate transient and dynamic processes [15,16]. For example, Klein [17] has formed a PV/T design in the TRNSYS software called type 50. In the literature, several types were exhibited to illustrate were introduced on how the product transmissivity τ – absorptivity α was applied besides the calculation of thermal losses [18-22]. Also, these studies have emphasized the thermal behavior of the PV/T unit, on the other side; researchers have not treated electrical behavior in much detail. Therefore, this work highlighted the general behavior aiming to increase the electrical-power output of the photo-voltage unit.

1 Experimental Strategy and Mathematical model of PV/T Unit.

The unit contains one identical separated pair of PV solar photovoltaic panels. The highest power at the output is 60W with rated current and voltage 2.61A, and 23V, respectively, and the panel's dimensions of $0.44m^2$. Regarding the design, the first panel is composed of two systems. The first was manufactured so that a film of water ran over its top shell made with no front glass, while the other system was utilized to exploit the generated heat by the panel. On the other hand, the second-panel work as a traditional unit. Figures 1a and b show the system under investigation and showing the water tube comes with a slit at the top of the PV panel, pumping system and the heat exchanger.

The next paragraph shows an illustration of how the system works. The water is distributed in a thin film after being pumped through the slit by a pump machine working with 0.25 HP, the inflow velocity is 1 lit/min. Another tiny tube comes with fins that work as a heat interchanger and consumer of heat acquired by the water and also operates as heat dispersion maintaining the heat degree at a constant level. Note that the water will be at the required temperature upon inflow to the panel surface.

In this work, the load of (8.7 Ω) was adopted aiming to obtain the highest value of power at the output. Next, using an Omega-type millimeter device the current and voltage were recorded with the accuracy of 1 mill ampere and 1 millivolt, respectively. The angle degree of panels is mounted to face the south direction at 45°. At the same slop of panels, the Kimo SL100 solar meter device (use for measuring the irradiance) was mounted at the corner of one of two panels. Additionally, the ambient heat was recorded in the shaded area over a systematic time. Also, to measure the upper/lower heat of the panels, Patch-model thermocouples (k-model) were employed. For more convenience, it used a surface probe to measure the upper side heat degree of the panel. The recorded heat value was 1.5 ^{O}C, which was higher than that of the back of the panel.

Thus, was adopted 1.5 ^{O}C was a heat value difference between them. Using thermocouples (k type) fixed at the finned tube end, the heat degree of the water prior to moving over the panel and the water heat degree is sticking out of the heat interchanger. Every 10 minutes, the data was collected over the period of 30 days in Baghdad, May 2022 (latitude 33.34^{o} and longitude 44.1^{o}). The next hypotheses were adopted to form the energy balance equation based on each PV/T solar collector element. The first is ignoring the heat capacity of the PV/T collector, and the second, owing to the constrained condition of the procedure, heat stratification in the water of the reservoir was excluded, third, the thermal distribution was considered to be constant over the entire system.

The losses due to the resistance were ignored as it was very small. Also, we used ηo as an indication of total efficiency as this symbol is communally utilized in the literature upon calculation of the PV/T performance [19].

$$\boldsymbol{\eta_o = \eta_t + \eta_e} \quad (1)$$

Where ηt and ηe are, the thermal and electric production efficiency of the PV/T unit, respectively. Take into consideration that electric power is higher than thermal power. The inflow rate parameter (FR) is taking the form:

$$\mathbf{F_r = 1 - e^{\frac{U_L F A_m}{C_f m \cdot}\left(\frac{m \cdot C_f}{U_L A_m}\right)}} \quad (2)$$

The solar-panel complex competence, F', gives the following formula

$$F' = \frac{1}{\frac{W}{FW-FD+D}+\frac{W_x U_L}{Dh\pi}} \quad (3)$$

a)

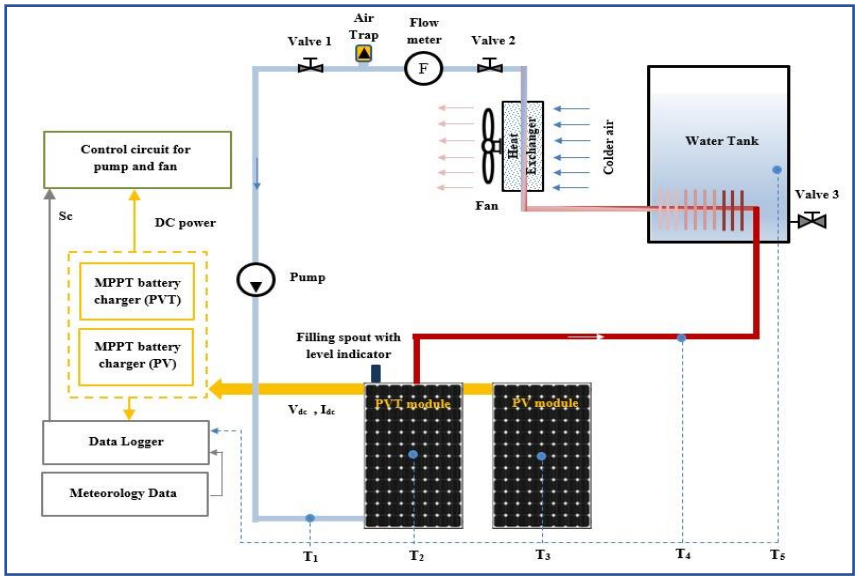

b)

Fig. 1. Pumping system of empirical integrated Photovoltaic/Thermal (PV/T) design:
a) – photo; b)- scheme

F represents the fin competence, and it takes the formula below

$$F = \frac{\tanh\frac{(W-D)\sqrt{U_L/K\sigma}}{2}}{\frac{(W-D)\sqrt{U_L/K\sigma}}{2}} \quad (4)$$

The general heat-losing parameter (UL) and thermal competency of the PV/T unit (ηt) take the expression below:

$$U_L = \frac{\eta_c I_c + I_c \alpha\tau}{T_a + T_c} \quad (5)$$

According to the defined variables

$$\eta_c = F_R\tau\alpha - F_R U_L \frac{T_a - T_{fi}}{I(t)} \quad (6)$$

The electric competency relies on the heat degree of the PV unit and the cell heat degree (Tc) is given in the expression below.

$$\eta_e = \eta_h(1 - \beta_o T_h - 25\beta_o) \quad (7)$$

$$T_c = T_a + \left(\frac{I(t)\tau\alpha}{U_L}\right)\left(\frac{1-\eta_c}{\tau\alpha}\right) \quad (8)$$

Where the transmission-absorption parameter τα and the general HT factor U take the expression below 0.86 and 0.8 W/m^2°C, respectively [19].

2 Results and Discussions

This section explains the outcome of these discussions. As it was mentioned earlier, the data were collected in May 2022. Figure 2 presents the variation in solar intensity gathered by the panels' surface. The greater the solar intensity, the higher the heat level, as illustrated in Figure 3.

In Figure 3, red curve shows radiation, blue curve presents cell temperature of PV, and green curve presents cell temperature of PVT. It was noted that the increase in radiation quantity from PV/T and PV units led to increasing the heat degree by 1.2C and 5.4C for the photovoltaic/thermal and photovoltaic units, respectively. Furthermore, it was discovered that on May 25, at 12:00, the highest point of the temperature of the photovoltaic module was 65 °C, while it was 32 °C for the photovoltaic/thermal module, and that it then decreased. And the cell temperature has been maintained in the range of 20–30 °C.

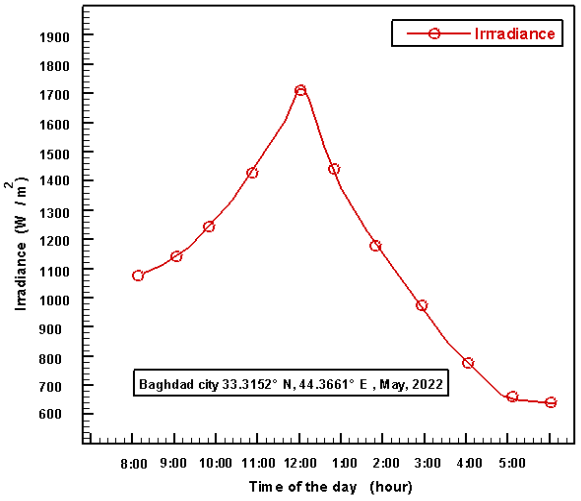

Fig. 2. Variation of irradiance over 24 hours.

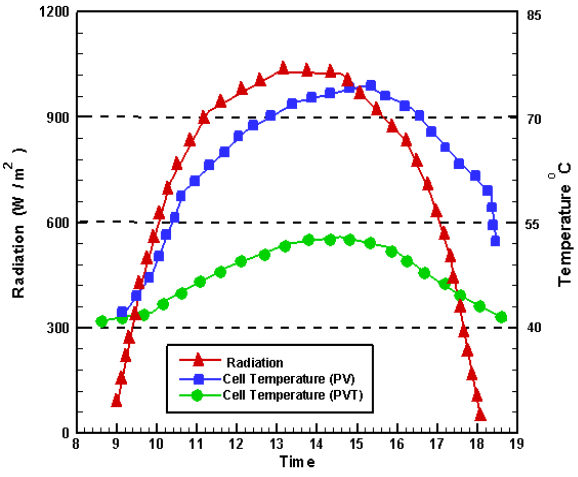

Fig. 3. Solar intensity and cell heat level of PV and PV/T

Furthermore, the results indicated that photovoltaic or thermal systems provided approximately 0.09% of the energy savings for various MFRs. This indicates that such a system has greater efficiency than traditional solar energy modules. In general, several factors can influence PV/T performance. For example, electrical and thermal transformation is influenced by parameters such as MFR, inlet and outlet water heat degrees, solar irradiance, the surrounding temperature, wind acceleration, and system orientation concerning the solar ray. On the other hand, the higher the temperature, the greater the decrease in unit efficiency. For instance, increasing the temperature by 3C led to a 0.2% decrease in efficiency. Even more, the experimental results demonstrated that higher electric conversion occurred at 55 °C and 1700 W/m^2, as shown in figure 4.

Furthermore, for various inflow rates, the electric efficiency ranges between 7 and 9 per cent. For instance, when the inflow rate is 0.004 kg/sec, the efficiency of the model is between 6 and 8 per cent, as shown in Figure 5. Regarding thermal efficiency, for various inflow rates, the value ranges from 20.67% to 110.67%. For example, the thermal efficiency was 60.67% and the average was 63.43%, while the lowest average efficiency was 50.03% for the MFR of 0.8 kg/sec.

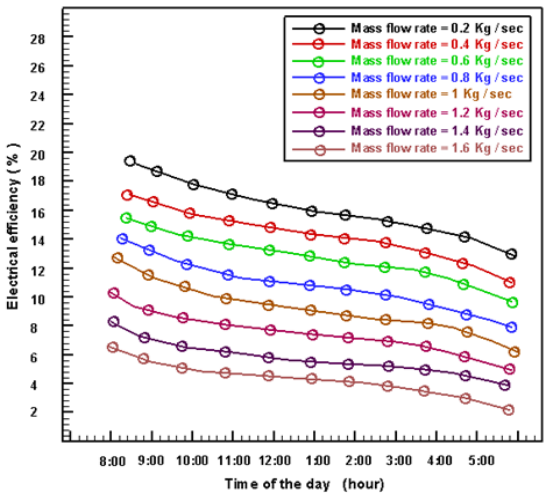

Fig. 4. Differentiation of Electrical Efficiency for different mass inflow rate for PV/T.

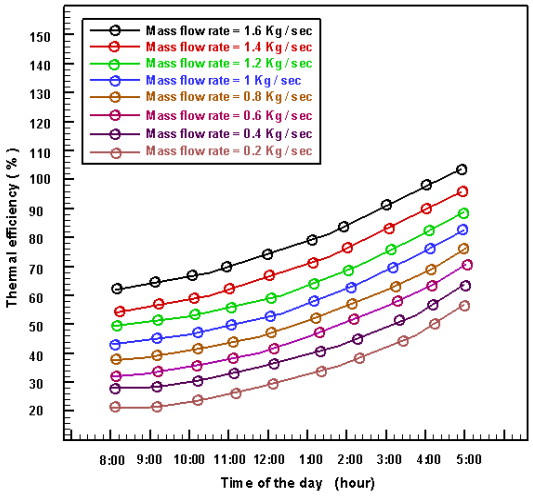

Fig. 5. Differentiation of thermal Efficiency for different mass inflow rate for PV/T

Concerning the entire efficiency, which represents the total electrical and thermal efficiency, Figure 6 depicts the photovoltaic/thermal performance. As can be seen, the range is 60.39% to 80.95% for different inflow velocities. In this context, the highest value exceeded 78.45% for a MFR of 0.8 kg/sec, and the lowest average overall efficiency was seen to be 59.67%.

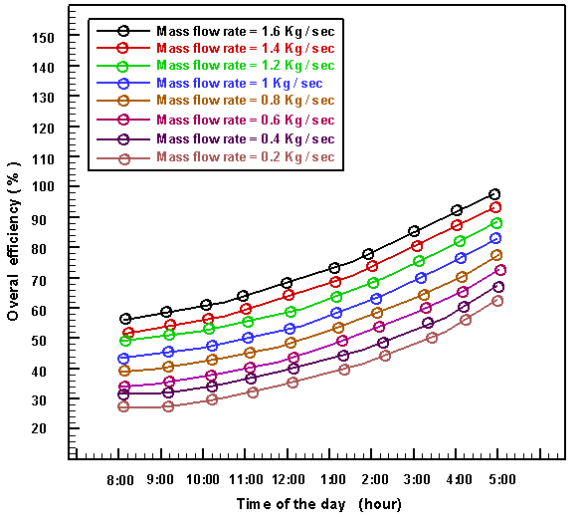

Fig. 6. Differentiation of Overall Efficiency for various mass inflow speeds for PV/T

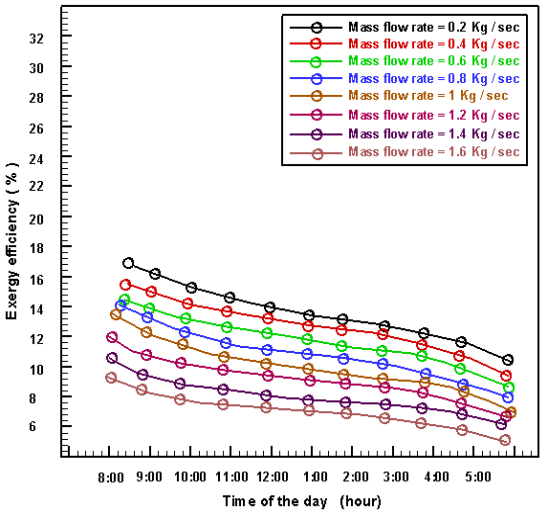

Fig. 7. Differentiation of Exergy Efficiency for various mass inflow speeds for PV/T

The difference in energy competency of photovoltaic and thermal for various MFRs of water. For different MFRs, the energy competency of photovoltaic and thermal systems ranges from 6.34% to 17.65%. The highest exergy efficiency was seen at 11.13% for a MFR of 0.8 kg/sec, as shown in Figure 7.

Figure 8 provides a comparison between different inflow rates in terms of energy-saving savings from solar PV/T. From the figure, it can be observed that the efficiency ranges from 30.35% to 90.45%, with the highest energy-saving efficiency reaching 50.34% for a MFR of 1 kg/sec. Figure 9 depicts the different heat degrees between the photovoltaic/thermal unit's inlet and outlet water temperatures (T_{fi}-T_{fo}) and for MFRs ranging from 0.2 kg/s to 1.6 kg/s various solar intensity quantities.

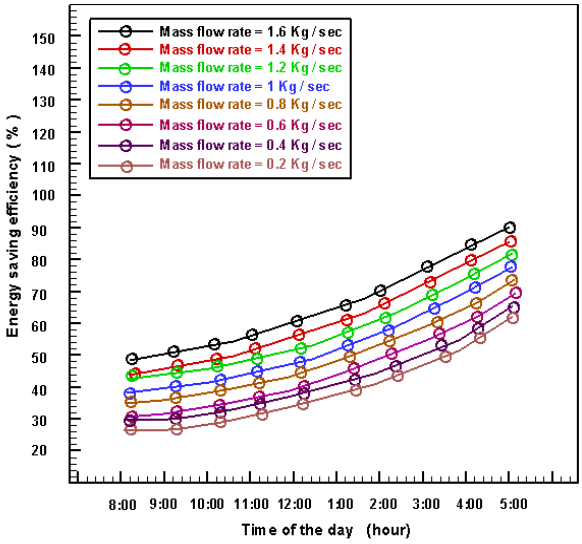

Fig. 8. Differentiation of Energy Saving Efficiency for different mass inflow rates for PV/T.

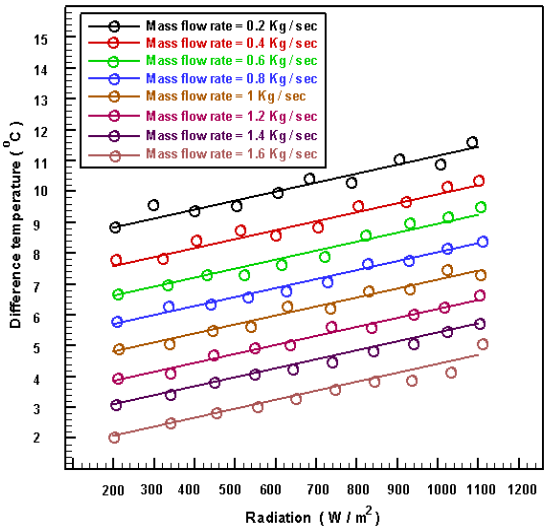

Fig. 9. Temperature variation of PV/T water collector with various inflow rates and irradiance

Further, the change in temperature of solar radiation temperature from 2 °C to 4 °C caused a change in the inlet and outlet temperatures, consequently causing a change in MFRs from 0.2 kg/s to 1.6 kg/s, respectively, at each 100 W/m^2. As can be observed, the higher the radion intensity, the higher the difference in temperature, and the higher the average inflow rate. Table 1 depicts the relationship between radiation intensity and temperature differences.

It is worth mentioning that the photovoltaic heat degree ranges between 50°C and 66°C, and for photovoltaic/thermal units, ranges between 40°C and 70°C at the solar intensity of 1700 W/m².

Table 1. Thermal competency expression of PV/T collector.

Mass inflow rate (kg/s)	Expression
0.2	$\eta_t = 0.32 - 2.362 \times \Delta T / I_t$
0.4	$\eta_t = 0.42 - 3.652 \times \Delta T / I_t$
0.6	$\eta_t = 0.51 - 4.821 \times \Delta T / I_t$
0.8	$\eta_t = 0.63 - 5.345 \times \Delta T / I_t$
1	$\eta_t = 0.72 - 6.23 \times \Delta T / I_t$
1.2	$\eta_t = 0.81 - 7.341 \times \Delta T / I_t$
1.4	$\eta_t = 0.93 - 8.589 \times \Delta T / I_t$
1.6	$\eta_t = 1.23 - 9.912 \times \Delta T / I_t$

As depicted in Figure 10, the efficiency of these two systems was 10.64% and 18.75%, respectively. In this vein, it can be concluded that PV/T efficiency outperforms the PV unit by 23.36%. The total electric product of both modules was 1300 W/m^2 and 1700 W/m^2, respectively. On the other hand, the entire solar intensity was 7450 W/m^2 on the test day. Figure 11 presents the whole electric efficiency produced by these two modules, which was 18.2% and 12.5%, respectively. In Figure 11, red curve shows electricity generated (PVT), blue curve presents radiation, and green curve presents electricity generated (PV). In comparison, 6% of energy production by PV/T is higher than that by PV module. The same scenario has been recorded at

13:00 for both modules. Finally, good agreement was found between the theoretical and experimental results; the differentiation could only be attributed to the losses in the cable and device errors.

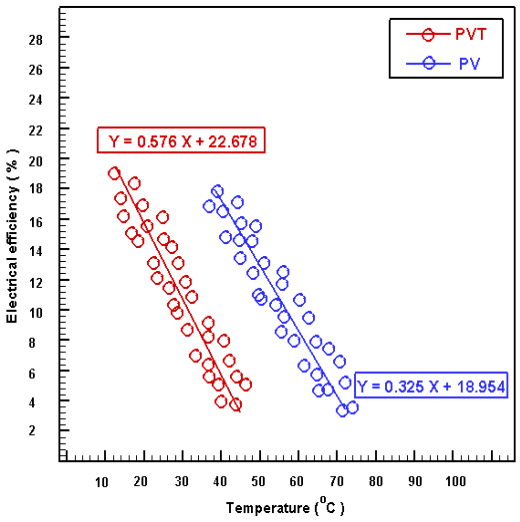

Fig.10. Differentiation of electrical competency against cell heat point for PV and PV/T at 1700 W/m^2 solar radiation hypothesis scenario.

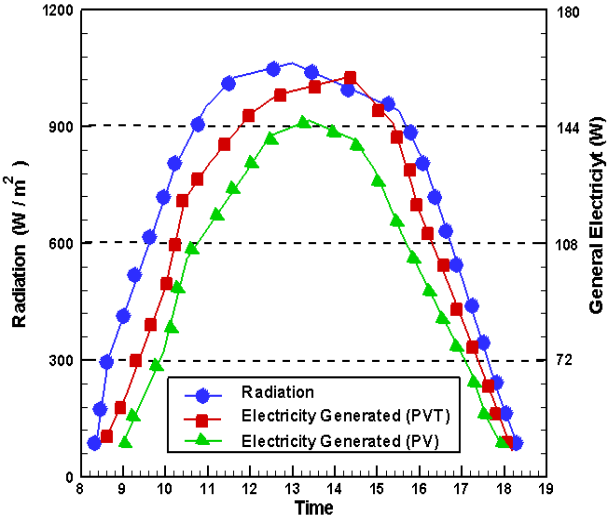

Fig.11. Electric production by PV and PV/T modules.

Conclusion

The most obvious finding to emerge from this study is that the module PV/T provides better-performing PV units, where the highest efficiency of the electrical system was 18.2%. This is demonstrated by the whole efficiency that arose from the PV/T system: 50–80% for the MFR of 0.2 kg/s with an efficiency of 22%. Also, with an MFR of 1 kg/s, the exergy efficiency ranges from 8% to 22%. The highest average exergy efficiency measured for the MFR of 0.8 kg/s was 10.64%. Concerning thermal performance, it was found that the highest value of thermal efficiency was 60%. The average efficiency increases as the MFR increases compared to the PV unit. Using the active cooling method, the PV efficiency is 12.5 per cent; thus, it provides an indication of promising results at 70 °C and the MFR of 0.2 kg/s. Both modules have similar behaviour in terms of electric generation. Finally, the amount of PV/T was 11300 W/m^2 compared to 1700 W/m^2 for the PV module, and the whole solar intensity was 7450 W/m^2 per 24 hours on May 25, 2022.

REFERENCES

1 Xu, L., Luo K., Ji J., Yu B., Li Z., Huang S. Study of a hybrid BIPV/T solar wall system. *Energy*, 2020, Vol.193, pp.116578. doi:10.1016/j.energy.2019.116578

2 Cao Y., Kamrani E., Mirzaei S., Khandakar A., Vaferi B. Electrical efficiency of the photovoltaic/thermal collectors cooled by nanofluids: Machine learning simulation and optimization by evolutionary algorithm. *Energy Rep.*, 2022, Vol.8, pp. 24–36. doi:10.1016/j.energy.2019.116578

3 Sohani, A., Dehnavi, A., Sayyaadi, H., Hoseinzadeh, S., Goodarzi, E., Garcia, D.A., Groppi, D. The real-time dynamic multiobjective optimization of a building integrated photovoltaic thermal (BIPV/T) system enhanced by phase change materials. *J. Energy Storage*, 2022, Vol.46, 103777. doi:10.1016/j.solener.2022.01.036

4 Jabber, Kadhim M., AL-Saadi, Mohammed K., Jaddoa Ameer A., Economic Operation of Smart Distribution Microgrid, *AIP Conference Proceedings*, 2022, 2415, 020027. doi:10.1063/5.0092301

5 Mahdi, Mahmoud M., Jaddoa, Ameer A., Al Ezzi Amged. Impact of pumping head on a solar pumping system with an optimal pv array configuration: solar water heater application, *Journal of Engineering Science and Technology*, 2022, Vol. 17, No. 3, pp. 2035 – 2048. doi:10.1007/978-981-15-2780-7_78

6 Mahdi, Mahmoud M., Jaddoa, Ameer A.. An experimental optimization study of a photovoltaic solar pumping system used for solar domestic hot water system under iraqi climate, *Journal of Thermal Engineering*, 2021, Vol. 7, No. 2, Special Is. 13, pp. 162-173. doi: 10.18186/thermal.871296.

7 Jabber, Kadhim M., AL-Saadi, Mohammed K., Jaddoa Ameer A., Economic Operation of Low Voltage Smart Micro-grid with Integration of Renewable Energy, *Engineering and Technology Journal*, 2022. Vol.40, No.07. doi:10.30684/etj.2022.131063.1000

8 Sattar M., Rehman A. Ahmad N., Mohammad A., Al Ahmadi A.A., Ullah N. Performance Analysis and Optimization of a Cooling System for Hybrid Solar Panels Based on Climatic Conditions of Islamabad, Pakistan. *Energies*, 2022, Vol. 15, 6278. doi:10.3390/en15176278

9 Hengel F., Heschl C., Inschlag F., Klanatsky P. System efficiency of pvt collector-driven heat pumps *Int. J. Thermofluids.*, 2020,pp. 5–6, Article 100034, doi: 10.1016/j.ijft.2020.100034

10 Alshibil A.M.A., Víg P., Farkas I. Performance evaluation of a hybrid solar collector in two different climates Eur. *J. Energy Res*., 2021, pp. 17-20. doi:10.24018/ejenergy.2021.1.2.11

11 Sakellariou, Axaopoulos, E.P. An experimentally validated, transient model for sheet and tube PVT collector Sol. *Energy*, 2018, Vol.174 pp. 709-718, doi:10.1016/j.solener.2018.09.058

12 Ul Abdin, Rachid Z.A., Bond graph modeling of a water-based photovoltaic thermal (PV/T) collector Sol. *Energy*, 2021, Vol. 220, pp. 571-577. doi:10.1016/j.solener.2021.03.028

13 Haloui H., Touafek K., Khelifa A. Modeling of a hybrid thermal photovoltaic (PVT) collector based on thin film organic solar cells Electr. *Power Syst. Res.*, 210 2022, Article 108131. doi:10.1016/j.epsr.2022.108131

14 Chaibi Y., El Rhafiki T., Simón-Allué R., I. Guedea, Luaces C., Charro Gajate O., Kousksou T., Zeraouli Y. Physical models for the design of photovoltaic/thermal collector systems. Sol. *Energy*, 2021,Vol. 226, pp. 134-146. doi:10.1016/j.solener.2021.08.048

15 Rashad M., Żabnieńska-Góra A., Norman L., Jouhara H., Analysis of energy demand in a residential building using TRNSYS. *Energy*, 2022,Vol. 254, 124357. doi:10.1016/j.energy.2022.124357

16 Davidsson H., Perers B., Karlsson B., System analysis of a multifunctional PV/T hybrid solar window Sol. *Energy*, 2012, Vol.86 , pp. 903-910. doi:10.1016/j.solener.2011.12.020

17 Klein S.A. Calculation of flat-plate collector loss coefficients Sol. *Energy*, 1975, Vol.17, pp. 79-80. doi:10.1016/0038-092X(75)90020-1

18 Klein SA, et al. TRNSYS reference manual, standard component library overview in: TRNSYS 16, a TRaNsient Syst. Simul. Progr., *University of Wisconsin*, Madison, 2006, pp. 3-93. http://sel.me.wisc.edu/trnsys

19 Ozgoren M., M. Aksoy H., Bakir C., Dogan S. Experimental Performance Investigation of Photovoltaic/Thermal (PV-T) System. *Conferences 1106,* 2013. 45, published by EDP Sciences. doi:10.1051/epjconf/20134501106

20 Omarova Zh., et al,. Performance Simulation of Eco-Friendly Solar Cells Based On $Ch_3nh_3sni_3$. *Eurasian Physical Technical Journal,* 2022, Vol.19, No. 2(40). doi: 10.31489/2022No2/58-64

21 Aimukhanov A.K., et. al., Influence of Phthalocyanine Nanostructures on Optical and Photovoltaic Characteristics of a Polymer Solar Cell. *Eurasian Physical Technical Journal*, 2022, Vol.19, No.1 (39), doi:10.31489/2022No1/26-33

22 Syzdykov A.B., et al. Algorithm For Finding Maximum Power Point Tracking when shadowing or failure of solar panel photo cells on satellites using low orbits. *Eurasian Physical Technical Journal*, 2023, Vol.20, No.1 (43), doi:10.31489/2023No1/65-72.

Nomenclature

A_m	Area of PV module	U_L	Overall heat loss coefficient ($W/m^2\ ^oC$)
C_f	Fluid specific heat (kcal/kg ^oC)	W	Width of the tube spacing (m)
D	Diameter of copper tube (m)	α	Absorptivity of glass
F	Fin efficiency factor	β_0	PV temperature coefficient ($^0C^{-1}$)
F`	Flat plate collector efficiency factor	δ	Plate thickness (m)
F_R	Flow rate factor	ΔT	Temperature difference (^oC)
ṁ	Fluid flow rate (kg/m^3)	η_t	Thermal efficiency of PV/T collector
T_{fi}	Fluid inlet temperature (^oC)	η_0	Overall efficiency of PV/T collector
T_{fo}	Fluid outlet temperature (^oC)	ηe	Electrical efficiency
T_c	PV cell temperature (^oC)	ηc	PV cell efficiency
T_a	Ambient temperature (^oC)	τ	Transmissivity of glass

Article accepted for publication 13.05.2023